
Article:
Sullivan, M.V. orcid.org/0000-0002-1771-8268, Clay, O., Moazami, M.P. et al. (2 more authors) (2021) Hybrid aptamer-molecularly imprinted polymer (aptaMIP) nanoparticles from protein recognition—a trypsin model. Macromolecular Bioscience, 21 (5). 2100002. ISSN 1616-5187

https://doi.org/10.1002/mabi.202100002

Macromolecular Bioscience
www.mbs-journal.de

Hybrid Aptamer-Molecularly Imprinted Polymer (aptaMIP) Nanoparticles from Protein Recognition—A Trypsin Model

*Mark V. Sullivan, Oliver Clay, Michael P. Moazami, Jonathan K. Watts, and Nicholas W. Turner**

Aptamers offer excellent potential for replacing antibodies for molecular recognition purposes however their performance can compromise with biological/environmental degradation being a particular problem. Molecularly imprinted Polymers (MIPs) offer an alternative to biological materials and while these offer the robustness and ability to work in extreme environmental conditions, they often lack the same recognition performance. By slightly adapting the chemical structure of a DNA aptamer it is incorporated for use as the recognition part of a MIP, thus creating an aptamer-MIP hybrid or aptaMIP. Here these are developed for the detection of the target protein trypsin. The aptaMIP nanoparticles offer superior binding affinity over conventional MIP nanoparticles (nanoMIPs), with K_D values of 6.8 $\times 10^{-9}$ ($\pm 0.2 \times 10^{-9}$) M and 12.3 $\times 10^{-9}$ ($\pm 0.4 \times 10^{-9}$) M for the aptaMIP and nanoMIP, respectively. The aptaMIP also outperforms the aptamer only (10.3×10^{-9} M). Good selectivity against other protein targets is observed. Using surface plasmon resonance, the limit of detection for aptaMIP nanoparticles is twofold lower (2 nM) compared to the nanoMIP (4 nM). Introduction of the aptamer as a "macro-monomer" into the MIP scaffold has beneficial effects and offers potential to improve this class of polymers significantly.

1. Introduction

The molecular recognition of large biomolecules such as nucleic acids, viruses, and proteins, has become increasingly topical, especially with the aim of developing sensors for the detection of disease markers.[1] There are numerous options available to researchers. The most well-known of these are antibodies which are well known for their use in analytical, diagnostic, and therapeutic applications, due to their strong affinity to target molecules.[2,3] Though, while these have many beneficial traits, they have several disadvantages, including elevated cost, animal-based sourcing, immunogenicity as well as limited shelf life and stability. As such, the drive for antibody replacements has led to interest in the development of suitable alternatives.[4,5]

One such alternative that has some significant commercial and academic interest is the aptamer. These small single-stranded RNA or DNA oligonucleotides[6] create internally folded 3D structures that are able to bind to molecules with great affinity and specificity through electrostatic interactions, hydrophobic interactions, and their complementary 3D shapes.[7] They have been shown to bind to a variety of molecular targets such as small molecules, proteins, nucleic acids as well as cells, tissues, and organisms. Due to their relatively accessible synthetic process, flexibility in design, and excellent molecular interaction profile, they have found use in biotechnological and therapeutic applications.[8,9] They offer advantages over antibodies because they are readily produced by chemical synthesis; possess desirable storage properties and elicit little or no immunogenicity in therapeutic applications.[6] Despite this, they do have some limitations, nominally around their thermal and chemical stability—the nature of the nucleic acid sequence leaves it open to degradation.

Another molecular recognition alternative is that of molecular imprinting.[10] Molecularly imprinted Polymers (MIPs) are gaining in popularity (in both commercial and academic settings) due to their performance characteristics including high affinity and selectivity, flexibility in applications, and resistance to extremes of temperature, pressure, and pH variations.[11,12] The process of generating a MIP involves the formation of

Dr. M. V. Sullivan, O. Clay, Dr. N. W. Turner
Leicester School of Pharmacy
De Montfort University
The Gateway, Leicester LE1 9BH, UK
E-mail: nicholas.turner@dmu.ac.uk
Dr. M. P. Moazami, Dr. J. K. Watts
RNA Therapeutics Institute
UMass Medical School
Worcester, MA 01605, USA
Dr. M. P. Moazami, Dr. J. K. Watts
Department of Biochemistry and Molecular Pharmacology
UMass Medical School
Worcester, MA 01605, USA
The ORCID identification number(s) for the author(s) of this article can be found under https://doi.org/10.1002/mabi.202100002.

DOI: 10.1002/mabi.202100002

selective sites in a polymer matrix. This usually involves the self-assembly of functional monomers around a template, through covalent and non-covalent bonds. The resultant template-monomer complexes are subsequently copolymerized with a suitable crosslinker. Removal of the template molecule from the polymer results in the formation of specific binding cavities, complementary in terms of structure and functionality to the template molecule.[13–15] For several years MIPs were limited by high levels of heterogeneity and by synthetic methods, but significant advances in molecular modeling and understanding of polymer chemistry have countered these issues.

Imprinting of proteins is especially attractive, as the potential for non-biological molecular recognition can overcome some of the inherent issues of using biological materials (immunoresponse, enzymatic degradation, etc.). They can also be targeted effectively for purpose, however there are some downsides as highlighted by Turner.[10] These include mass transfer, flexibility and stability of target, and heterogeneity when imprinting larger templates. Modern imprinting methods are able to overcome these.

The development and enhancement of molecularly imprinted polymeric nanoparticles (nanoMIPs) have opened new perspectives in nanotechnology. These have attracted a lot of attention due to their flexibility and analytical performance. These materials have the potential to transform traditional analytical methods in chemistry, biochemistry, environmental sciences, and biomedical fields.[16,17]

The synthesis of hybrid materials, which exhibit the benefits of both aptamers and nanoMIPs, and in doing so, reduces the negative traits of both, is of great interest. From an aptamer point-of-view, materials that maintain biological level recognition capabilities of an aptamer, while protecting the nucleic acid oligonucleotide from degradation would be highly sought after, while from a MIP viewpoint the use of a specific targeted "monomer" that can reduce heterogeneity would improve the

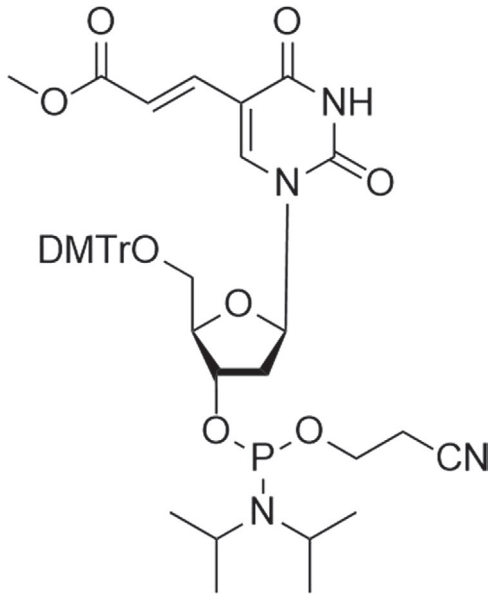

Figure 1. Replacement thymine base. Modified Carboxy-dT-CE Phosphoramidite (**T***).

performed of this valuable class of artificial recognition material. Several groups have considered this as discussed in an excellent short review by Zhang and Liu.[18]

For example, Spivak and team used Acrydite-linked small aptamers in a hydrogel to act as a biomolecular-responsive capture agent. When the template was present the gel "shrunk" signifying binding.[19] Jolly et al. (2016) used a 5′-thiolated sequence, bound to gold electrode. Around the aptamer-template complex a polydopamine scaffold was formed.[20] With admirable detection limits they showed that the fixed sequence with its polymer offered threefold improvement of affinity when compared to the aptamer alone.

This work mirrors the 2014 findings of the Turner group who created the first true aptamer-MIPs (aptaMIPs), where the aptamer was used as a "macro-monomer." Here the thymine bases in a sequence were replaced by a carboxy-dT (**Figure 1**). The sequence specific for cocaine was then used in the creation of nanoMIPs which already exhibit exceptional binding capabilities. Not only did the binding affinity when compared to the free aptamer increase by three orders of magnitude, the aptaMIP performance was an improvement on the plain nanoMIP. This was hypothesized to be due to the use of multiple-point linkages holding the aptamer into an optimal binding conformation. This multiple-linker strategy has also been employed by Allabush who used it to incorporate an aptamer into a gel for protein electrophoresis.[21] Incorporation of an aptamer into a hybrid system in this manner also has shown to increase stability,[22] and counter any thermal or enzymatic (nuclease) degradation that is often seen with aptamers on their own.[23,24]

The aim of this study is to further explore the development of hybrid-MIP nanoparticles (aptaMIP NP) for a protein target (trypsin). Prior to this paper, the technique had only been demonstrated using short nucleic acid sequences[25] or small molecules[22] as discussed in the previous paragraph. Using similar chemistry as these papers, we now employ a superior analytical technique, (that of surface plasmon resonance (SPR), which offers greater sensitivity when compared to the microgravimetric measurements previously used) to compare the performance of these aptaMIPs against nanoMIPs, and the published data of the free aptamer to determine any improvement in affinity/specificity. Selectivity of the hybrid is also examined with reloading of a non-target protein (lysozyme and bovine serum albumin (BSA)).

2. Results and Discussion

2.1. Preparation and Characterisation

Here we present a novel strategy for the preparation of soluble aptaMIP nanoparticle hybrid for the protein trypsin. The procedure of the solid-phase synthesis of trypsin-specific aptaMIP NPs was adapted from the protocols of Safaryan and Poma.[22,26] The target protein is attached to a solid support, with the aptaMIP NPs then being synthesized onto the solid support, which is easily released, thanks to their thermoresponsive properties. The strategy is schematically presented in **Figure 2**. The glass beads (diameter 75 μm) were first silanized with (3-aminopropyl)trimethoxysilane (APTMS) and the protein

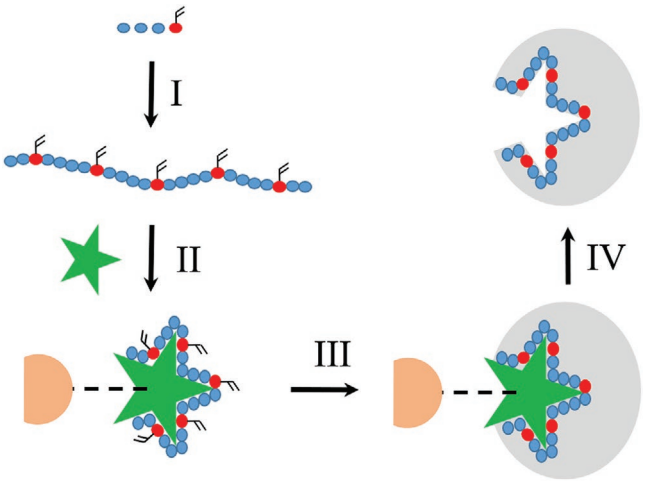

Figure 2. Schematic representation of the solid-phase synthesis of aptaMIP NPs. Red circle indicates the modified polymerizable base. Green Star representative of trypsin protein. I) Synthesis of modified aptamer sequence. II) Complexation of aptamer with protein target attached to inert solid phase. III) Addition of polymer scaffold components, polymerization, and formation of polymer scaffold via TEMED initiated reaction; IV) Thermal (60 °C) release of nanoparticle bearing aptamer sequence. Note: protein template is left affixed to support for re-use. Note: Positive control nanoMIPs made using same solid-phase method as shown[27], but without the aptamer present.

(trypsin) was attached using glutaraldehyde (GA) as a coupling agent. The polymerizable aptamer was then incubated with the protein derivatized glass beads to form a protein-aptamer complex, with polymerization conducted around the immobilized complex. *N*-Isopropylacrylamide (NIPAm) was used as the major component in the polymer recipe, which enables thermoresponsive properties in the resultant NPs. Corresponding plain MIP nanoparticles were produced, for comparison, using the same method, but with the absence of the polymerizable aptamer. These will be known as aptaMIP and nanoMIP forthwith.

The aptamer (5′-GACAGCCACATGTACTGAGGTA-GACTTGGGTGGGGGACAG-3′) specific for trypsin was produced with a modified with a carboxy polymerizable functional group (shown in Figure 1). These modified bases are shown in bold, within the sequence. The aptamer is modified with six anchoring points, where previous studies[22] have shown that multiple anchoring points provide the best rebinding performance. Given that multiple-linkers sites were shown to be beneficial we did not elect to study single-point linkers at 5′ or 3′ ends. This is in line with prior work,[22] which showed that a single modification at either end was not effective in fixing the aptamer into the polymer in an effective manner. We elected to not put two modifications together position 26–27) as it is not clear what effect this might have on the oligo structure. Likewise, having two polymerizable modifications next to each other may hinder reactivity.

The concentration of the aptaMIP and nanoMIP nanoparticle solutions were calculated to be 58 ± 10 μg mL^{-1} and 114 ± 18 μg mL^{-1}, respectively. In order to determine this concentration, 3 mL of sample was incubated at 60 °C until dry, particle mass was measured (6-point balance) and concentration (per mL) was calculated. The aptaMIP and nanoMIP materials were then analyzed by dynamic light scattering (DLS) and scanning electron microscopy (SEM). They showed a diameter of 219 ± 8 nm and 107 ± 6 nm at 25 °C, respectively (see Figures S1 and S2, Supporting Information, ESI, for particle distribution and the SEM images). The differences in size are interesting and have been noted in prior studies. Given that the polymerization conditions (and length of reaction) are the same, we might expect the sizes to be similar, however these data suggest there may be another factor. One potential hypothesis is that the aptamer in its optimal binding conformation interacting with the template during pre-complexation offers a superior nucleation site when compared to the random orientation of the monomers in the nanoMIP reaction. This is under investigation.

2.2. Binding Performance of Proteins to Synthesised Imprinted Nanoparticles

The nanoparticles were then dissolved into the running buffer solution, with the addition of sodium acetate, for SPR analysis. A carboxymethyl dextran hydrogel-coated Au chip was activated using *N*-hydroxysuccinimide (NHS) and 1-Ethyl-3-(3-dimethylaminopropyl)carbodiimide (EDC), followed by the addition of the dissolved NP. The functionality on the polymer scaffold reacts allowing the nanoparticles to covalently link to the chip surface. Finally, a quenching solution of ethanolamine was used to deactivate the carboxyl group and wash away any unbound NP.

The sensorgrams of the interactions of the five different concentrations of the same target protein (trypsin) captured by the aptaMIP (**Figure 3**A) and nanoMIP (Figure 3B), immobilized on the sensor surface. 0.01% Tween20 was added to the running buffer to reduce non-specific binding.

To study cross-reactivity and non-specific binding, non-target proteins (Lysozyme and BSA) were also investigated. The binding for lysozyme is shown in Figure 3C (aptaMIP) and Figure 3D (nanoMIP) and the binding for BSA is shown in Figure 3E (aptaMIP) and Figure 3F (nanoMIP). Experiments were repeated in triplicate and the SPR curves were fitted to a 1:1 interaction model. The overall equilibrium dissociation constant (K_D) of the aptaMIP and nanoMIP toward these proteins were determined. This is summarised in **Table 1**.

The method to produce the nanoMIP materials was adapted from the work of Safaryan, which also successfully produced nanoMIPs for trypsin with an estimated K_D value of 15.8 nM.[26] The nanoMIPs produced within this study have a calculated K_D valued of 12.3 nM (Table 1). These two are comparable and as such confirm the validity of the synthetic technique. The nanoMIP, without the addition of a specific monomer, offers binding and recognition toward the target protein[26] comparable to published antibodies and the free aptamer that was used in this experiment.[28,29]

The K_D of the interaction between trypsin and the trypsin-specific aptaMIP hybrids has been calculated at 6.8 nM (Table 1). The fixing of the aptamer into the scaffold of the MIP improves the K_D twofold (6.8 versus 12.3 nM), when compared to the nanoMIP, made in the same way but without the macromonomer. While this is not as dramatic an increase as observed

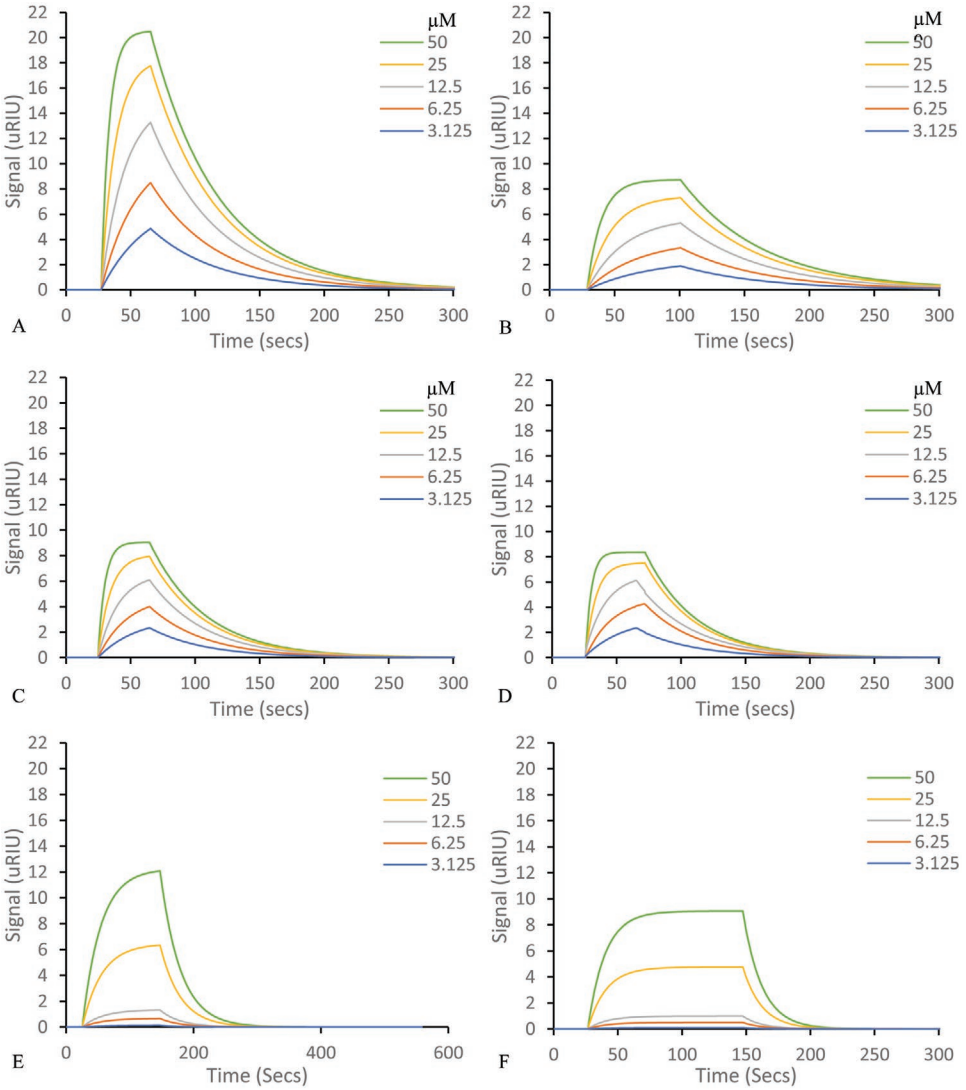

Figure 3. Representative SPR sensorgrams of molecular interactions of various nanoparticles immobilized on carboxymethyl dextran hydrogel coated Au chips, to solutions containing five concentrations of protein (trypsin, lysozyme, or BSA, with lysozyme or BSA as negative controls). A) Trypsin binding to trypsin-imprinted aptaMIPs; B) trypsin versus trypsin-imprinted nanoMIPs; C) lysozyme binding to trypsin-imprinted aptaMIPs; and D) lysozyme binding to trypsin-imprinted nanoMIPs. E) BSA binding to trypsin-imprinted aptaMIPs; and F) BSA binding to trypsin-imprinted nanoMIPs.

in prior work (namely the 2000× increase observed in Poma's work,[22] the initial aptamer selected here already had superior affinity properties (nM affinity compared to μM in the cocaine aptamer in the prior Poma work). This validates the approach used and supports the observation that the addition of a pre-targeted macro-monomer improves performance. The ratio of relative signal strengths (Figure 3) shows the aptaMIP offers approximately double the signal upon binding compared to the nanoMIP. This is relative to the ratio of $K_{D\ aptaMIP}/K_{D\ nanoMIP}$ which is 1.80. The comparison is expected as it suggests that the aptaMIP consistently binds more material at a given concentration, supporting it having greater affinity.

Work by Xiao showed this trypsin aptamer to have the lowest calculated dissociation constant (K_D) value of 10.3 nM and has been used further by Wang for the immobilization of trypsin onto modified silica particles.[28,29] Mirroring the prior work by Poma, the suspension of the aptamer in the polymeric scaffold, through locking it into an optimal binding conformation, has increased the aptamer recognition performance. It is further evidence that fixing the aptamer in place in an optimal binding conformation increases performance through reducing entropic effects—the interaction is under thermodynamic control and by fixing less energy is lost to flexing and reorientation of the aptamer. In essence it is shaped exactly as needed for optimal binding.

Also, this aptamer has a sequence of 5′TTGGGTGGGGG-3′, which has the potential for transformation into a G-quartet, whereby the G-quartet can play a pivotal role in the binding mechanism of aptamers.[30–32] This is interesting given that two modifications were placed within this motif which suggests that complex secondary structure can be modified without disruption of binding.

Table 1. Calculated equilibrium dissociation constant (K_D) of imprinted materials.

	K_D [M]		
	Trypsin	Lysozyme	BSA
aptaMIP	6.8×10^{-9} ($\pm 0.2 \times 10^{-9}$)	5.4×10^{-6} ($\pm 0.4 \times 10^{-6}$)	7.6×10^{-6} ($\pm 1.1 \times 10^{-6}$)
nanoMIP	12.3×10^{-9} ($\pm 0.4 \times 10^{-9}$)	3.2×10^{-6} ($\pm 0.5 \times 10^{-6}$)	6.3×10^{-6} ($\pm 0.8 \times 10^{-6}$)

In order to evaluate the ability of the generated materials to discriminate between trypsin and other proteins, both the aptaMIP and nanoMIP were challenged with the non-imprinted proteins lysozyme, chosen due to the approximate size and hydrophobic solvent accessible surface areas (SASA) and BSA, chosen as it is a representative protein in the same matrix that trypsin may be found. SPR analysis, shown in Figure 3C–F reveals that there is some binding of lysozyme and BSA to both the materials, but with vastly reduced affinity (K_D values of 5.4, 3.2, 7.6, and 6.3 μM, respectively). This demonstrates that both systems, as expected, are selective for the template. The K_D value difference between the lysozyme or BSA binding in the aptaMIP and nanoMIP particles is similar, and the decrease observed also, further suggesting that any binding of lysozyme or BSA to the NPs is non-specific. The observed relative signal is comparable as well suggesting no differences in affinity. In summary, the nanoMIP has less affinity for the target template, but higher cross-reactivity when compared to the aptaMIP, suggesting that the aptaMIP is the superior material.

The aptaMIP and nanoMIP detection limits were investigated in order to determine the lower limit of detection (LOD) for both the aptaMIP and nanoMIP particles. SPR analysis was conducted using a concentration range of 0.001–1 μM and the curves are shown in **Figure 4**. Eight different concentrations of the same target protein (trypsin) were captured by the aptaMIP (Figure 4A) and nanoMIP (Figure 4B), which were immobilized on the sensor surface. A 0.01% Tween20 was added to the running buffer to reduce non-specific binding. Using the maximum signal (μRIU) from the fitted curves, concentration calibrations were plotted. This allowed for the estimation of the theoretical lower LOD.

The aptaMIP produced a lower LOD estimate of 2.4 nM, while the nanoMIP produced a lower LOD estimate of 4.1 nM. These estimates show that the identical sensor surfaces coated with aptaMIP particles are able to detect lower concentrations of the target molecule, compared with the nanoMIP. The ratio $LOD_{nanoMIP}/LOD_{aptaMIP}$ is 1.70 and is comparable to the $K_{D\ aptaMIP}/K_{D\ nanoMIP}$ of 1.80 (Table 1). It should be noted the obtained signal here is relative, and the scale is not comparable to Figure 3. This is an artifact of the software and experimental setup. Given the synthetic protocol is the same, and results are replicable, this suggests the aptaMIP particles have superior binding affinities over the nanoMIP which further supports that the addition of the "macro-monomer" aptamer is beneficial to the imprinting process, improving not just affinity and specificity (Table 1) in comparative applications. Therefore, they are demonstrably superior materials in sensor applications. While these data differences may look small, in analytical terms a doubling of performance is significant and can be the difference between a positive or negative result. This is also in the magnitude observed by Jolly.[20]

Overall the data presented here further supports the use of a targeted predetermined "macro-monomer" in the synthesis of imprinted materials. It agrees with prior data, from this group and others that the hybrid approach offers a good opportunity to improve MIP performance.

3. Conclusion

By combining bio-recognition oligonucleotides (aptamers) with molecularly imprinted materials, we are able to demonstrate a hybrid material that exhibits superior performance to its components—a material that is greater than the sum of its parts. This was observed both in terms of their affinity toward the template protein, but also in cross-reactivity studies. The synthesis of these materials is relatively straightforward using an existing solid-phase synthesis methodology. The gentle polymerization conditions allow for the aptamer monomers and protein template to retain their stability, eradicating any potential denaturation during the polymerization process. These hybrid systems targeting proteins could lead the way for potential sensor applications as demonstrated in this communication. Given the improvements observed here, these materials could have significant potential in therapeutic applications. Multiple opportunities exist with a variety of targets and alterations to the chemistry involved. Potential changes to the running buffer (increase in surfactant) or longer equilibrium periods may further reduce cross-reactivity, and are under investigation. We are currently exploring position and number of linkers to elucidate what is required to maintain an effective incorporation and imprint. We are also exploring the potential of using these materials in sensor applications.

Several questions still remain with these nascent hybrids, including that of nucleation around the aptamer appearing to alter the polymerization reaction kinetics; and how to further reduce non-specific binding, but the authors expect in time these questions will be answered. What is clear is that there is a future for these hybrid materials in the fields of both imprinted polymers and aptamers.

4. Experimental Section

Materials and Equipment: N-(3-Dimethylaminopropyl)-N′-ethylcarbodiimide (EDC), (3-aminopropyl)trimethyloxy-silane (APTMS), acrylic acid, ammonium persulfate (APS), dipotassium phosphate, Bovine Serum Albumin (BSA), disodium phosphate, ethanolamine, ethylenediaminetetraacetic acid, glass beads, glutaldehyde, glycine, lysozyme, *N,N′*-methylenebisacrylamide (BIS), N-Hydroxysuccinimide (NHS), N-Isopropylacrylamide (NIPAm), *N-tert*-butylacrylamide (TBAm), sodium dodecyl sulfate (SDS), Tween 20, tetramethylethyldiamide (TEMED), and trypsin were all purchased and used without purification

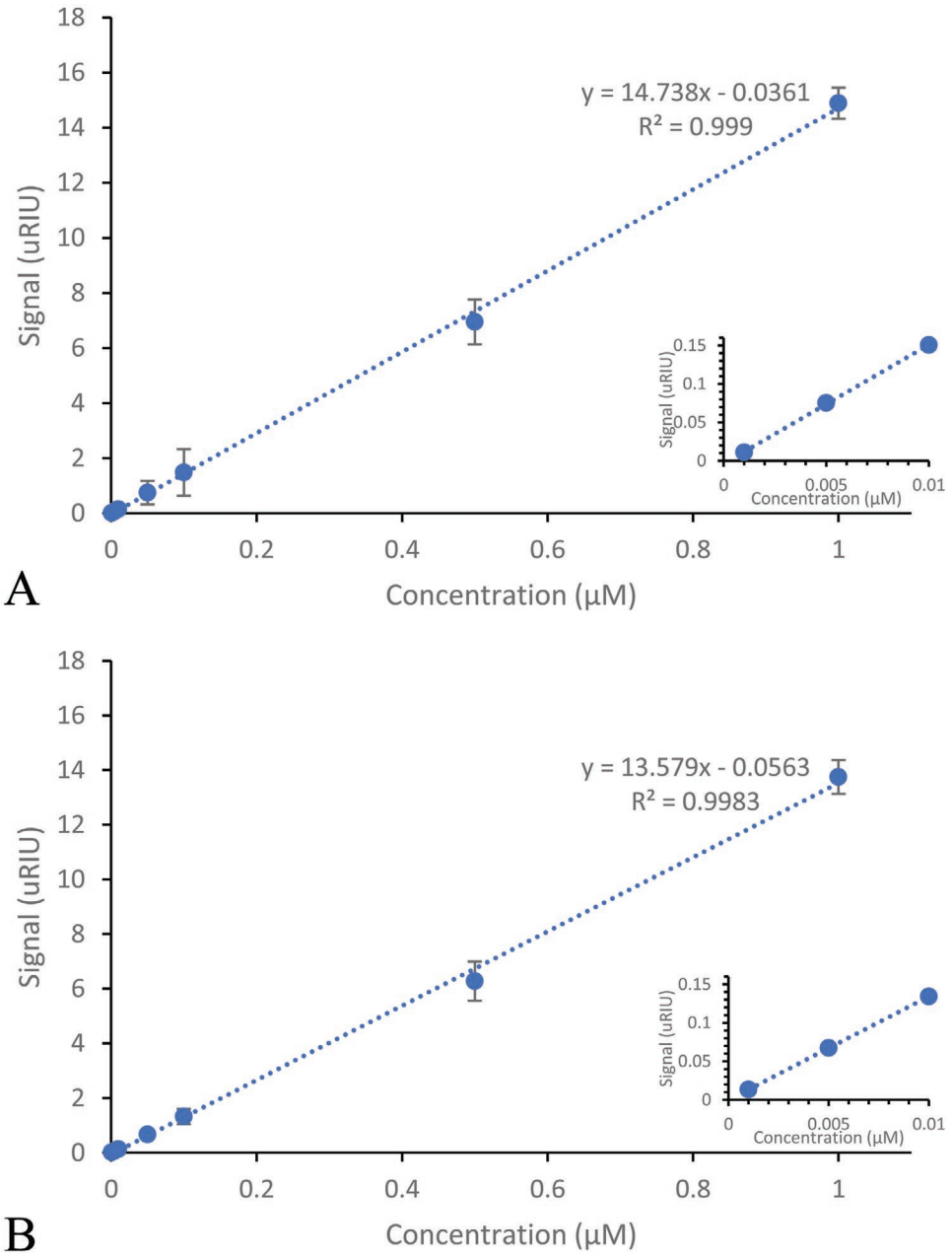

Figure 4. Elucidation of limit of detection for SPE sensor. Relative signal versus concentration. A) Trypsin binding to trypsin-imprinted aptaMIPs concentration calibration (insert showing linearity of the low concentration range); B) trypsin binding to trypsin-imprinted nanoMIPs concentration calibration (insert showing linearity of the low concentration range).

from Sigma Aldrich, Poole, Dorset, UK. Acetone, acetonitrile (dry), methanol, potassium chloride, and sodium hydroxide were all purchased and used without purification from Fisher Scientific UK Ltd, Loughborough, UK. Carboxy-dT-CE phosphonamidite was purchased and used without purification from LGC Link, Bellshill, Lanarkshire, UK. Double-distilled water was used for the analysis. All chemicals and solvents were analytical or high-performance liquid chromatography (HPLC) grade and were used without further purification. Trypsin aptamer sequence was selected for use based on this literature.[28,29]

Synthesis of Polymerizable Aptamer Sequence: The trypsin aptamer (5′-GACAGCCACA**T**GT**T**AC**T**GAGG**T**AGAC**T**TGGG**T**GGGGGACAG-3′) (where T in bold represents the insertion of a polymerizable base **T***) was synthesized under standard conditions at 10-µmol scale on an AKTA Oligopilot 10 oligonucleotide synthesizer. The oligomers were briefly treated with diethylamine, then deprotected and released from the support by treatment with concentrated aqueous NH_3 at 55 °C for 16 h. The solutions were concentrated to dryness, resuspended in water, and desalted using NAP-10 columns (GE Healthcare). Oligonucleotide masses were verified using an Agilent 6530 QTOF LC/MS system.

Preparation of Trypsin-Derivatized Glass Beads as Affinity Media: Glass beads (30 g, 75 µm diameter, Supelco) were activated by boiling in 4 M NaOH (24 mL) for 15 min, then washed thoroughly with double-distilled water (eight times with 100 mL, for 30 g of beads), until the pH of the water/bead solution was around 7. Rinsed twice with acetone (100 mL) and dried at 80 °C for 3 h. They were then incubated in a 12 mL solution of APTMS (3%, v/v) in anhydrous toluene overnight at 60 °C. After

incubation the glass beads were washed with 8 volumes (100 mL) of acetone, followed by 2 volumes (100 mL) of methanol, and dried in an oven at 150 °C for 30 min. The amine-functionalized beads were then incubated in a 7% (v/v) GA solution (0.5 mL of solution per gram of beads) for 2 h at room temperature. Trypsin (7.5 mg at 0.5 mg mL^{-1}) was introduced to the GA-modified beads in 15 mL phosphate-buffered saline (PBS, 10 mM) pH 7.4, with the solution being left to incubate at room temperature overnight, sealed under nitrogen. The trypsin derivatized beads were washed thoroughly with doubled-distilled water and dried under vacuum. After this step, the glass beads were used straight away for the synthesis of the imprinted nanoparticles without further storage.

Solid-Phase Synthesis of Trypsin Imprinted nanoMIPs: A polymerization mixture consisting of NIPAm (20 mg). BIS (1 mg), and AA (2.2 µL) in 49 mL of double distilled water, was produced. In a separated vial 17 mg of TBAm was dissolved in 250 µL of ethanol and this was added to the previous solution with the other compounds. Finally, double distilled water was added to the flask with the polymerization mixture to adjust the total volume to 50 mL. This solution was degassed under vacuum, while sonicating for 10 min. Following this, the polymerization mixture was bubbled for 20 min with a slow stream of N_2.

Meanwhile, 30 g of the template-derivatized glass beads were transferred into a 100 mL sealable bottle and degassed by purging with N_2 for 10 min. Next, the 50 mL of degassed solution of monomers was poured onto the glass beads, followed by the rapid addition of 12.5 µL of TEMED and 15 mg of APS dissolved in 250 µL of double distilled water, to allow for polymerization to be initiated. Everything was gently agitated via swirl motion and left to polymerize for 1 h at room temperature, gently swirling from time to time. Note it is important that this is gentle to limit risk of abrasion. After the synthesis, the beads were filtered through a 11 µm filter paper, using gravity filtration and then the beads were washed 8 × 30 mL of water at ambient temperature in order to remove the impurities, unreacted monomers, and low-affinity nanoMIPs. To elute high affinity nanoMIPs, the beads were heated in 40 mL of water at 60 °C, then filtered again using gravity filtration, the beads were then further washed with volumes of 20 mL of water at 60 °C until ≈100 mL of the eluted nanoparticles in water was collected. The solutions of all nanoMIPs were stored at 4 °C until measurements were taken.

Solid-Phase Synthesis of Trypsin Imprinted Hybrid-MIPs: In different vials, a solution of 1.74 µmol of the aptamer in 10 mL of double distilled water was prepared and a polymerization mixture consisting of NIPAm (20 mg), BIS (1 mg), and AA (2.2 µL) in 39 mL of double distilled water was prepared. In a separated vial 17 mg of TBAm was dissolved in 250 µL of ethanol and this was added to the previous solution with the other compounds. Finally, double distilled water was added to the flask with the polymerization mixture to adjust the total volume to 40 mL. This solution was degassed under vacuum, while sonicating for 10 min. Following this, the polymerization mixture was bubbled for 20 min with a slow stream of N_2.

Meanwhile 30 g of the template-derivatized glass beads were transferred into a 100 mL sealable bottle and degassed by purging with N_2 for 10 min. The aptamer solution was poured onto the glass beads and left to incubate at room temperature for 10 min, with gentle swirling. Next, the 40 mL of degassed solution of monomers was poured onto the glass beads, followed by the rapid addition of 12.5 µL of TEMED and 15 mg of APS dissolved in 250 µL of double distilled water, to allow for polymerization to be initiated. Everything was swirled very gently and left to polymerize for 1 h at room temperature, gently swirling from time to time. After the synthesis, the beads were filtered through a 11 µm filter paper, using gravity filtration and then the beads were washed 8 × 30 mL of water at ambient temperature in order to remove the impurities, unreacted monomers, and low-affinity AptaMIP NPs. To elute high affinity AptaMIP NPs, the beads were heated in 40 mL of water at 60 °C, then filtered again using gravity filtration, the beads were then washed with volumes of 20 mL of water at 60 °C, until ≈100 mL of the eluted nanoparticles in water was collected. The solutions of all AptaMIP NPs were stored at 4 °C until measurements were taken.

Characterization of Nanoparticles: Effective hydrodynamic diameters (d_h) of the particles were determined by DLS with a NanoBrook Omni spectrometer (Brookhaven, United States) at 25 °C. Particle size was determined using Particle Solutions (v2.6) software with a total of 5 measurements per sample and a time interval of 10 s between measurements.

The shape and surface topography of the nanoparticles were determined by using Carl Zeiss SEM EVO High Definition 15 Scanning Electron Microscope (Carl Zeiss, Germany) operating at 15 kV. The samples were mounted on a metal stub with double-side adhesive tape and gold-coated under vacuum in an argon atmosphere prior to observation.

The concentration of the nanoparticle solution was calculated by taking 3 mL of the solution and evaporated to dryness at 60 °C. The mass of the dried particles was then measured, divided by three to reveal the concentration in µg mL^{-1}. This was repeated five times.

SPR experiments were performed in order to evaluate the affinity and specificity of the imprinted nanoparticles for the different targets. Measurements were carried out using a Reichert 2SPR system.

Immobilisation of the SPR Sensor Surface: Carboxymethyl Dextran Hydrogel coated Au chips, purchased from Reichert Technologies (Buffalo, USA) were installed onto a Reichert 2SPR following the manufacturer's instructions. The sensor surface was then preconditioned by running PBST (PBS pH 7.4 and 0.01% Tween 20) at 10 µL min^{-1} until a stable baseline was obtained. The flow rate of 10 µL was maintained throughout the immobilization process. In order to activate carboxy groups on the surface of the sensor chip, fresh preparation of 40 mg EDC and 10 mg NHS dissolved in 1 mL water was injected onto the sensor chip surface for 6 min. To the activated surface 300 µg of the aptaMIP or nanoMIP dissolved in 1 mL of the running buffer (PBST) and 10 mM sodium acetate (820 µg mL^{-1}), (this was added in order to activate the NH functional groups within the MIP NP, this allows for the MIP NP to bind to the SPR chip surface), using NHS EDC coupling, the aptaMIP or nanoMIP solution was injected only to the left channel of the surface for 1 min (multiple NH_2 functionalities were available from the composition of the polymer scaffold). Finally, a quenching solution (1 M ethanolamine, pH 8.5) was injected for 8 min to deactivate carboxyl groups and to wash away the unbound nanoMIP. A continuous flow of running buffer (PBST) at 10 µL min^{-1} was maintained after the completion of the aptaMIP or nanoMIP immobilization. SPR assays were carried out after a stable baseline was achieved. The left channel was the working channel while the right channel was the reference.

Kinetic Analysis Using SPR: Kinetic analysis was initiated by injection of the running buffer PBST (blank) onto the aptaMIP/nanoMIP immobilized sensor surface for 2 min, followed by PBST for 5 min. The binding kinetics of an individual aptaMIP/nanoMIP to the selected target protein (trypsin) was determined from serial dilutions (five concentrations, 50–3.125 µM) of trypsin under study. Each dilution was injected for 2 min (association) followed by PBST for 5 min (dissociation). After dissociation, the target protein was removed from the immobilized surface by injecting regeneration buffer (10 mM Glycine-HCl, pH 2) for 1 min followed by PBST for 1 min. The same procedures were repeated for the remaining four dilutions of the protein. After the analyses were completed, signals from left channel were subtracted from signals from their respective reference channel (the right channel). Selectivity for the aptaMIP/nanoMIP particles was investigated by repeating the SPR kinetic analysis, but using two non-target proteins (lysozyme and BSA) at the same concentrations instead. All analyses were carried out at 25 °C.

The SPR responses from five concentrations of the target protein were fitted to a 1:1 bio-interaction model (Langmuir fit model) utilizing TraceDrawer Software. Association rate constant (k_a), dissociation rate constant (k_d), and maximum binding (B_{max}) were fitted globally, whereas the BI signal was fitted locally. The equilibrium dissociation constant (K_D) was calculated from the ratio k_d/k_a. A SPR sensorgram calibration was created using a concentration range of 0.001–1 µM and was used to calculate a lower LOD.

Supporting Information

Supporting Information is available from the Wiley Online Library or from the author.

Acknowledgements

M.V.S. and N.W.T. would like to thank EPSRC for financial support for this work (EP/K015095/1) and (EP/S003339/1). O.C. would like to thank Dr Rachel Armitage and Leonie Hough for support with SEM imaging.

Conflict of Interest

The authors declare no conflict of interest.

Data Availability Statement

The data that support the findings of this study are available from the corresponding author upon reasonable request.

Keywords

aptamers, molecularly imprinted polymers, nanoparticles, protein, solid-phase synthesis

Received: January 25, 2021
Revised: February 24, 2021
Published online:

[1] R. Gui, H. Jin, H. Guo, Z. Wang, *Biosens. Bioelectron.* **2018**, *100*, 56.
[2] O. Hayden, P. A. Lieberzeit, D. Blaas, F. L. Dickert, *Adv. Funct. Mater.* **2006**, *16*, 1269.
[3] T. S. Bedwell, M. J. Whitcombe, *Anal. Bioanal. Chem.* **2016**, *408*, 1735.
[4] P. Chames, M. Van Regenmortal, E. Weiss, D. Baty, *Br. J. Pharmacol.* **2009**, *157*, 220.
[5] V. J. B. Ruigrok, M. Levisson, M. H. M. Eppink, H. Smidt, J. Van Der Oost, *Biochem. J.* **2011**, *436*, 1.
[6] A. V. Lakhin, V. Z. Tarantul, L. V. Gening, *Acta Naturae* **2013**, *5*, 34.
[7] A. V. Kulbachinskiy, *Biochemistry (Moscow)* **2007**, *72*, 1505.
[8] A. V. Lakhin, A. A. Kazakov, A. V. Makarova, Y. I. Pavlov, A. S. Efremova, S. I. Shram, V. Z. Tarantul, L. V. Gening, *Nucleic Acid Ther.* **2012**, *22*, 49.
[9] S. Missailidis, A. Hardy, *Expert Opin. Ther. Pat.* **2009**, *19*, 1073.
[10] N. W. Turner, C. W. Jeans, K. R. Brain, C. J. Allender, V. Hlady, D. W. Britt, *Biotechnol. Prog.* **2006**, *22*, 1474.
[11] K. Mosbach, O. Ramstron, *Nat. Biotechnol.* **1996**, *14*, 163.
[12] H. El-Sharif, D. M. Hawkins, D. Stevenson, S. M. Reddy, *Phys. Chem. Chem. Phys.* **2014**, *16*, 15483.
[13] M. V. Sullivan, S. R. Dennison, G. Archontis, J. M. Hayes, S. M. Reddy, *J. Phys. Chem. B* **2019**, *123*, 5432.
[14] D. M. Hawkins, D. Stevenson, S. M. Reddy, *Anal. Chim. Acta* **2005**, *542*, 61.
[15] A. Poma, A. Guerreiro, M. J. Whitcombe, E. V. Piletska, A. P. F. Turner, S. A. Piletsky, *Adv. Funct. Mater.* **2013**, *23*, 2821.
[16] F. Canfarotta, A. Poma, A. Guerreiro, S. A. Piletsky, *Nat. Protoc.* **2016**, *11*, 443.
[17] A. Poma, A. P. Turner, S. A. Piletsky, *Trends Biotechnol.* **2010**, *28*, 629.
[18] Z. Zhang, J. Liu, *Small* **2019**, *15*, 1805246.
[19] W. Bai, N. A. Gariano, D. A. Spivak, *J. Am. Chem. Soc.* **2013**, *135*, 6977.
[20] P. Jolly, V. Tamboli, R. L. Harniman, P. Estrela, C. J. Allender, J. L. Bowen, *Biosens. Bioelectron.* **2016**, *75*, 188.
[21] F. Allabush, P. M. Mendes, J. H. R. Tucker, *RSC Adv.* **2019**, *9*, 31511.
[22] A. Poma, H. Brahmbhatt, H. M. Pendergraff, J. K. Watts, N. W. Turner, *Adv. Mater.* **2014**, *27*, 750.
[23] M. C. Rodriguez, A. Kawde, J. Wang, *Chem. Commun.* **2005**, *34*, 4267.
[24] J. Keum, H. Bermudez, *Chem. Commun.* **2009**, *45*, 7036.
[25] H. Brahmbhatt, A. Poma, H. M. Pendergraff, J. K. Watts, N. W. Turner, *Biomater. Sci.* **2016**, *4*, 281.
[26] A. H. M. Safaryan, A. M. Smith, T. S. Bedwell, E. V. Piletska, F. Canfarotta, S. A. Piletsky, *Nanoscale Adv.* **2019**, *1*, 3709.
[27] F. Canfarotta, S. A. Piletsky, N. W. Turner, *Methods in Molecular Biology* (Eds: J. Gerrard, L. Domigan), Humana, New York **2020**, pp. 183–194.
[28] P. Xiao, X. Lv, S. Wang, J. Iqbal, H. Qing, Q. Li, Y. Deng, *Anal. Biochem.* **2013**, *441*, 123.
[29] Y. Wang, X. Lv, Y. Li, G. Peng, J. Iqbal, Y. Deng, *Anal. Methods* **2016**, *8*, 4277.
[30] M. Fialova, J. Kypr, M. Vorlickova, *Biochem. Biophys. Res. Commun.* **2006**, *344*, 50.
[31] D. E. Huizenga, J. W. Szostak, *Biochemistry* **1995**, *34*, 656.
[32] E. Vianini, M. Palumbo, B. Gatto, *Bioorg. Med. Chem.* **2001**, *9*, 2543.